

Material stability analysis based on the local and global elasto-plastic tangent operators

Florent Prunier, Farid Laouafa, Félix Darve

► **To cite this version:**

Florent Prunier, Farid Laouafa, Félix Darve. Material stability analysis based on the local and global elasto-plastic tangent operators. 1. International Symposium on computational geomechanics (COM-GEO 2009), Apr 2009, Juan-les-Pins, France. IC2E. Rhodes, pp.215-225, 2009. <ineris-00973337>

HAL Id: ineris-00973337

<https://hal-ineris.archives-ouvertes.fr/ineris-00973337>

Submitted on 4 Apr 2014

HAL is a multi-disciplinary open access archive for the deposit and dissemination of scientific research documents, whether they are published or not. The documents may come from teaching and research institutions in France or abroad, or from public or private research centers.

L'archive ouverte pluridisciplinaire **HAL**, est destinée au dépôt et à la diffusion de documents scientifiques de niveau recherche, publiés ou non, émanant des établissements d'enseignement et de recherche français ou étrangers, des laboratoires publics ou privés.

MATERIAL STABILITY ANALYSIS BASED ON THE LOCAL AND GLOBAL ELASTO-PLASTIC TANGENT OPERATORS

Florent Prunier

Laboratoire Sols, Solides, Structures, Risques, Institut Polytechnique de Grenoble, France

Farid Laouafa

Unité Risques Naturels, Ouvrages & Stockages, INERIS, Verneuil en Halatte, France

Félix Darve

Laboratoire Sols, Solides, Structures, Risques, Institut Polytechnique de Grenoble, France

ABSTRACT: *The present paper investigates bifurcation in geomaterials with the help of the second-order work criterion. The approach applies mainly to non associated materials such as soils. The analysis usually performed at the material point level is extended to quasi-static boundary value problems, by considering the finite element stiffness matrix. The first part of the paper reminds some results obtained at the material point level. The bifurcation domain is presented in the 3D principal stress space as well as 3D cones of unstable loading directions for an incrementally nonlinear constitutive model. In the second part, the analysis is extended to boundary value problems in quasi-static conditions. Non-linear finite element computations are performed and the global tangent stiffness matrix is analyzed. For several examples the eigenvector associated with the first vanishing eigenvalue of the symmetrical part of the stiffness matrix gives an accurate estimation of the failure mode even for non homogeneous boundary value problems.*

1 INTRODUCTION

Prediction of failure in geomaterials has not yet been completely clarified. This paper proposes an original approach providing some tools that may help respond to this question. We restrict our analysis to problems involving only rate-independent materials, with emphasis on non associated pressure-dependent materials such as granular media. Phenomenological constitutive models describe the material behaviour, and boundary value problems are solved using finite element analysis.

One of the main features of geomaterials is nonassociativity: the normality rule is not fulfilled, and as a consequence the elastoplastic tensor loses its major symmetry (Hill 1967; Mandel 1966; Mróz 1963; Mróz 1966). Because of this physical and mathematical feature, it is now well known that failure can occur strictly within the plasticity boundary condition such as Mohr-Coulomb condition (Lade 1992; Nova 1991; Darve & Chau 1987; Darve & Vardoulakis 2004).

In order to analyze material instabilities, several criteria have been proposed. The criteria most often used by engineers are probably (1) the limit condition of plasticity, and (2) the strain localization condition proposed by Rice (1976) given by the vanishing value of the acoustic

tensor. However, the second-order work criterion constitutes a lower bound for these two criteria (Bigoni & Hueckel 1991).

Hill (1958) proposed the following sufficient condition of stability for an elastoplastic body:

$$\int_V \dot{s}_{ij} \frac{\partial \dot{u}_j}{\partial x_i} dV > 0 \quad \forall \left\| \frac{\partial \dot{u}_j}{\partial x_i} \right\| \neq 0 \quad (1)$$

where V is the volume of the body at time t , s_{ij} the component of the nominal stress tensor (the transpose of the first Piolat-Kirchoff tensor), and $\partial \dot{u}_j / \partial x_i$ the gradient velocity. In the case of a small strain assumption and by neglecting geometrical effects, the condition (1) reads:

$$\int_V d\sigma_{ij} d\varepsilon_{ij} dV > 0 \quad \forall \|d\varepsilon\| \neq 0 \quad (2)$$

with $d\sigma$ the incremental Cauchy stress tensor, and $d\varepsilon$ the incremental strain tensor. In the first section, this condition is analyzed at the material point level. Thus the expression investigated is:

$$d^2W = d\sigma_{ij} d\varepsilon_{ij} > 0 \quad \forall \|d\varepsilon\| \neq 0 \quad (3)$$

where d^2W is the second-order work and $d\sigma$ and $d\varepsilon$ are linked by their constitutive equation. Darve & Laouafa (2000) showed that what determines the effective instability (at a given stress-strain state) depends on the loading direction and the nature of the controlled loading parameters. We will show that elliptical cones of unstable loading directions (denoted "instability cone") exist. If after a given loading path, the incremental loading direction is included within one of these cones, failure can occur. We thereby define the limit of the bifurcation domain by the set of stress-strain states for which a unique unstable loading direction exists. Furthermore, as shown by Nova (1994), the nature of loading variables determines the effective failure. For instance, in an undrained triaxial test performed on a loose sand, the q peak can be reached and passed if the loading is strain controlled, whereas if the loading is axially force controlled, failure occurs because the sample can not sustain any increase of q .

In the following section, the limit of the bifurcation domain plotted in the 3D stress space is depicted for the incrementally nonlinear and incrementally piecewise linear constitutive relations from Darve (Darve, Flavigny, & Meghachou 1995). An analytical equation of the instability cones is given, and it is presented in the 3D principal stress space for both constitutive models.

In section 3, a stability analysis based on the features of the eigenvalues and eigenvectors of the symmetrical part of the global tangent stiffness matrix \underline{K}_s is performed. The boundary value problem of a shallow foundation lying on an axisymmetrical soil is then analyzed.

2 SECOND-ORDER WORK CRITERION ANALYSIS WITHIN A PHENOMENOLOGICAL FRAMEWORK

This section discusses the numerical and analytical analyses of the second-order work criterion at the material point level. These analyses use elastoplastic constitutive relations. If small perturbations are assumed, we can state that a material point of a body is stable (in Hill's understanding) if, for any $(d\sigma, d\varepsilon)$ linked by their constitutive relation, equation (3) is fulfilled. Hence equation (3) constitutes a sufficient, but not necessary, condition of stability. In the case where $d^2W \leq 0$, the effective collapse of a homogeneous sample depends on the loading direction and on the controlled loading variables, as mentioned above.

If we denote by $\underline{\underline{M}}$ the matrix such that $d\sigma = \underline{\underline{M}} d\varepsilon$ and by $\underline{\underline{N}}$ the matrix such that $\underline{\underline{M}} = \underline{\underline{N}}^{-1}$, the second order work vanishes when:

$${}^t d\varepsilon \underline{\underline{M}} d\varepsilon = 0 \Leftrightarrow {}^t d\varepsilon \underline{\underline{M}}_s d\varepsilon = 0 \quad (4)$$

or equivalently when:

$${}^t d\sigma \underline{\underline{N}} d\sigma = 0 \Leftrightarrow {}^t d\sigma \underline{\underline{N}}_s d\sigma = 0 \quad (5)$$

The constitutive equation can take the following form in a given tensorial zone¹ and if expressed in principal axes:

$$\begin{bmatrix} d\varepsilon_1 \\ d\varepsilon_2 \\ d\varepsilon_3 \end{bmatrix} = \begin{bmatrix} \frac{1}{E_1} & -\frac{\nu_{21}}{E_2} & -\frac{\nu_{31}}{E_3} \\ -\frac{\nu_{12}}{E_1} & \frac{1}{E_2} & -\frac{\nu_{32}}{E_3} \\ -\frac{\nu_{13}}{E_1} & -\frac{\nu_{23}}{E_2} & \frac{1}{E_3} \end{bmatrix} \begin{bmatrix} d\sigma_1 \\ d\sigma_2 \\ d\sigma_3 \end{bmatrix} \quad (6)$$

where E_i and ν_{ij} are, respectively, the tangent Young moduli and tangent Poisson's ratios. From equation (5), we obtain the following expression:

$$\frac{d\sigma_1^2}{E_1} + \frac{d\sigma_2^2}{E_2} + \frac{d\sigma_3^2}{E_3} - \left(\frac{\nu_{12}}{E_1} + \frac{\nu_{21}}{E_2} \right) d\sigma_1 d\sigma_2 - \left(\frac{\nu_{32}}{E_3} + \frac{\nu_{23}}{E_3} \right) d\sigma_3 d\sigma_2 - \left(\frac{\nu_{13}}{E_1} + \frac{\nu_{31}}{E_2} \right) d\sigma_1 d\sigma_3 = 0 \quad (7)$$

The left-hand side of equation (7) is a quadric, with neither constant terms nor terms of degree one according to $d\sigma_i$. Consequently, the solution of equation (7) is an elliptical cone if the quadric is not degenerated. The real nature of this solution depends on the positiveness of $\det(\underline{\underline{N}}_s)$ and the four cases displayed on Fig.1 can be considered. If we assume that the eigenvalues, $\lambda_1, \lambda_2, \lambda_3$, are positive at the virgin state and evolve continuously with the loading parameter, the limit of the bifurcation domain (defined by the set of stress-strain states for which a unique unstable loading direction exists) is obtained with the first vanishing value of $\det(\underline{\underline{N}}_s)$. This analysis is rigorously exact in the case of incrementally linear constitutive relations (i.e., linear or nonlinear hypoelasticity or hyperelasticity). In the case of elastoplastic models, solutions of equation (7) have to be looked for in each tensorial zone, and truncated if necessary. By denoting \underline{u}_0 the eigenvector associated with the first vanishing eigenvalue λ_0 , Z_j the tensorial zone where the computation is performed, and n the number of tensorial zones, the limit of the bifurcation domain is given by the following relation (Prunier, Nicot, Darve, Laouafa, & Lignon 2009):

$$\min_{i=1,\dots,n} \left(\det(\underline{\underline{N}}_s^i) \right) = \det(\underline{\underline{N}}_s^j) = 0 \text{ and } \underline{u}_0 \subset Z_j \quad (8)$$

Fig.2 shows the 3D bifurcation domain obtained with Darve's two constitutive models (Darve, Flavigny, & Meghachou 1995) and dense sand, and Fig.3 shows some 3D instability cones. These cones were obtained for stress states located along a drained triaxial test performed on dense Hostun sand. As a reminder, the octolinear model presents eight tensorial zones defined here by the three orthogonal principal stress planes. It is worth noting that these cones are situated before the plasticity limit, and their opening increases continuously with the loading parameter until plastic limit surface.

In conclusion, dual analyses (i.e. $d\sigma$ versus $d\varepsilon$ or $d\varepsilon$ versus $d\sigma$) can be performed without

¹ A tensorial zone is a domain of the loading space in which the incremental constitutive relation is linear (Darve & Labanieh 1982). A classical elastoplastic model has two tensorial zones: one for loading and another one for unloading.

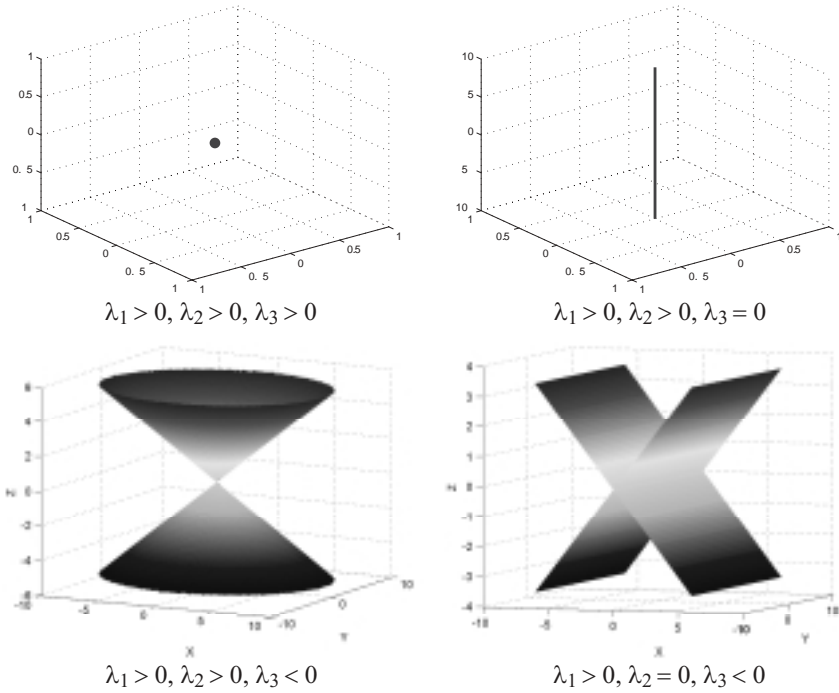


Fig. 1. Solutions of the equation: $\lambda_1 X^2 + \lambda_2 Y^2 + \lambda_3 Z^2 = 0$.

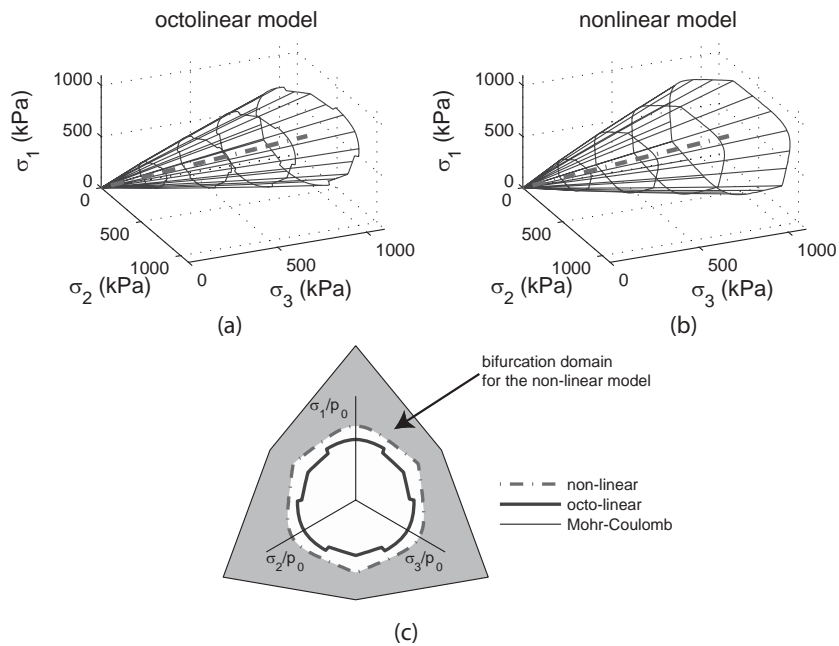


Fig. 2. Bifurcation domain plotted with octo and nonlinear models for dense Hostun sand. (a) corresponds to the limit of the bifurcation domain for the octilinear model, and (b) for the nonlinear model. (c) is the cut of these domains by the deviatoric plane.

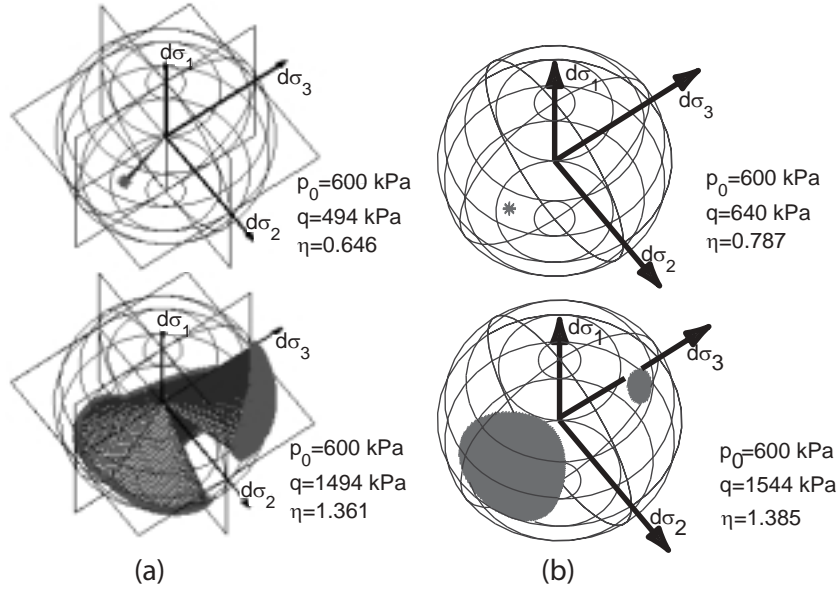


Fig. 3. 3D cones of unstable stress direction for dense Hostun sand. (a) presents the cones obtained with the octolinear model. The planes represent the limit between the eight tensorial zones, the meshes correspond to the analytical solution and the points cloud the solution obtained with the numerical method. (b) shows the results obtained with the nonlinear model using the numerical method (no analytical result is available). p_0 is the initial confining pressure, $q = \sigma_1 - \sigma_3$, $\eta = \frac{q}{p}$.

any restriction on the constitutive tensor because of the strict equivalence between equation (5) and equation (4). For the limit plastic condition characterized by $\det(\underline{\underline{M}}) = 0$, it happens that:

$$\det(\underline{\underline{M}}) = 0 \neq \det(\underline{\underline{N}}) = 0 \quad (9)$$

But the equivalence is maintained for the symmetrical part of these matrices:

$$\det(\underline{\underline{M}}_s) = 0 \Leftrightarrow \det(\underline{\underline{N}}_s) = 0 \quad (10)$$

In fact it can be shown that (Prunier, Laouafa, & Darve 2009):

$$\det(\underline{\underline{M}}_s) = \frac{\det(\underline{\underline{N}}_s)}{(\det(\underline{\underline{N}}))^2}, \quad (11)$$

In the case of associated materials, $\underline{\underline{M}}_s = \underline{\underline{M}}$ and $\underline{\underline{N}}_s = \underline{\underline{N}}$. Equation (11) gives $\det(\underline{\underline{M}}) = 1/\det(\underline{\underline{N}})$ and remains true, but equation (10) is no longer valid. The limit plastic condition can never be expressed in a dual manner by considering $\underline{\underline{M}}$ or $\underline{\underline{N}}$ indifferently.

3 ANALYSIS OF THE FINITE ELEMENT TANGENT STIFFNESS MATRIX

As seen in the previous section, the spectral analysis of the symmetric part of the constitutive matrix provides an interesting way to analyze bifurcation at the material point level. The aim of this section is to check whether the same analysis done on the global tangent stiffness matrix

leads to the same conclusion. The result presented below is the solution of a nonlinear boundary value problems, under the quasi-static assumption. The finite element code *Lagamine* (Lagamine 2007) developed at Liège University is used in the computations. The constitutive model considered in this code is an elastoplastic frictional pressure-sensitive relation developed for granular media (Barnichon 1998). It is based on the Van Eekelen (1980) yield criterion, it takes into account soil hardening, and the flow rule is non associated.

However it is not because some material points of a body are unstable that the global collapse actually occurs. In other words, local instability at some material points does not necessarily imply global instability. That is why it is necessary to consider the expression of the second-order work (equation (1)) integrated onto the whole body.

The relation between the integrated second-order work (D^2W) and the tangent stiffness matrix $\underline{\underline{K}}$ is as follows (Prunier, Laouafa, Lignon, & Darve 2009):

$$D^2W = \int_V d^2W dV = {}^t dU \underline{\underline{dF}} = {}^t dU \underline{\underline{K}} dU = {}^t dU \underline{\underline{K_s}} dU \quad (12)$$

with $\underline{\underline{dF}}$ and $\underline{\underline{dU}}$ the global vectors of the incremental force and of the incremental displacement, respectively. This result makes analyzing the symmetrical part of $\underline{\underline{K}}$ (denoted $\underline{\underline{K_s}}$) pertinent.

The heuristic problem presented hereafter is the one of a shallow foundation resting on a soil body. The foundation is simulated by a pressure acting on the soil surface. Geometrical data, boundary conditions as well as the deformed mesh at the divergence of the computation are shown in Fig.4. Nodal displacements at the bottom are totally fixed, while lateral displacements

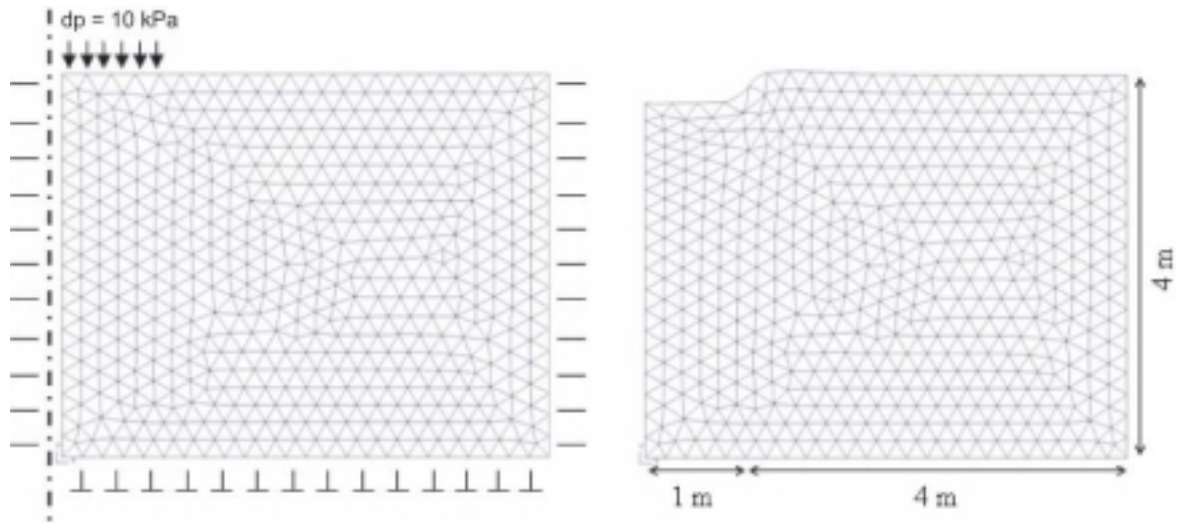


Fig. 4. Description of the geometry and the boundary conditions of the problem. dp is the increment of stress applied at each computation step.

are fixed only in the horizontal direction. The main parameters of the soil are displayed in Table 1.

Fig.5 presents the changes in the lowest eigenvalues of $\underline{\underline{K_s}}$. This lowest eigenvalue Λ_0 vanishes at step 25, long before the divergence of the computation at step 41. Since Λ_0 vanishes, a loading direction in term of global displacement increment $\underline{\underline{dU}}$ may exist for which global failure can be expected. But this loading direction does not necessarily match the loading direction imposed at the boundaries of the problem. Furthermore, Fig.6 shows that Λ_0 vanishes even before

Table 1. Main parameters of the soil body

E	ν	ρ	C	ϕ	ψ
95 MPa	0.21	2740 kg/m ³	30 kPa	15°	0°

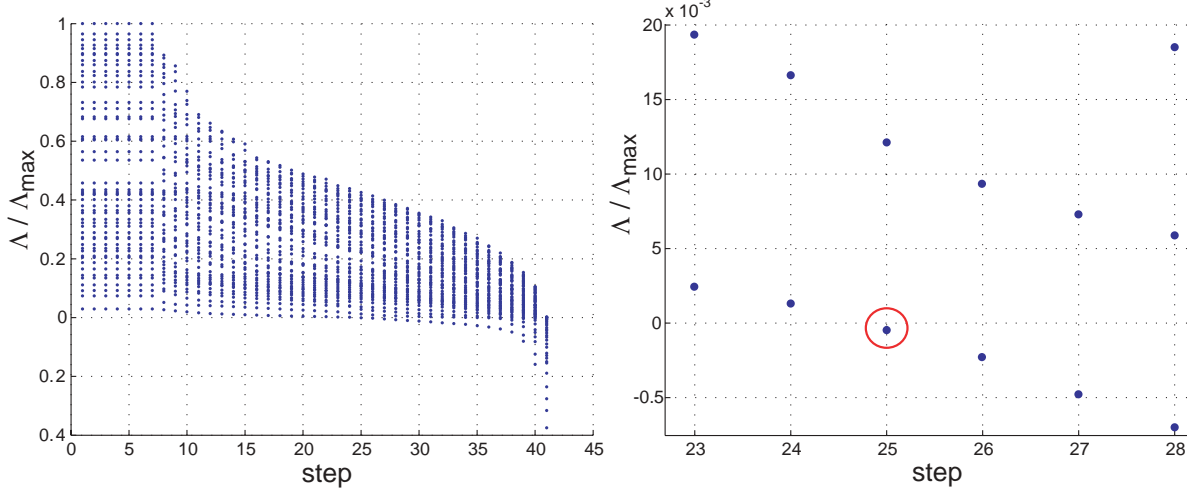


Fig. 5. The smallest eigenvalues of $\underline{\underline{K}}_s$ versus computation steps. On the right hand-side is a zoom around the first vanishing eigenvalue.

the first vanishing value of d^2W_n at one of the integration points. Hence, knowing the change in eigenvalues of $\underline{\underline{K}}_s$ can be valuable when the structure is potentially unstable, while the changes in d^2W_n at each integration point gives the evolution in weakness zones along the loading program considered until the global collapse.

As for the eigenvector of $\underline{\underline{K}}_s$, we denote by \underline{V}_0 the one linked to the first vanishing eigenvalue Λ_0 , and by \underline{dU}_f the incremental global displacement observed at the last converged step. Fig.7 presents the qualitative deviation between \underline{V}_0 and \underline{dU}_f . As a reminder, for homogeneous cases (the discussion is based on the analysis of the constitutive tensor), the eigenvector associated with the first vanishing eigenvalue of $\underline{\underline{M}}_s$ or $\underline{\underline{N}}_s$ gives the current flow rule, which characterizes the potential failure mechanism. Furthermore, in the case of the present elastoplastic model, it was observed that this direction plotted in the strain space is relatively close to the ultimate flow rule (Prunier, Laouafa, Lignon, & Darve 2009). The figure Fig.7 shows that this result is also qualitatively verified in this simulation. Quantitatively, we define the following function to measure the deviation between the directions of any two vectors (\underline{V}_1 and \underline{V}_2) of \mathbb{R}^n :

$$er(\underline{V}_1, \underline{V}_2) = \left(1 - \left| \frac{{}^t\underline{V}_1 \cdot \underline{V}_2}{\|\underline{V}_1\| \cdot \|\underline{V}_2\|} \right| \right) \cdot 100 \quad (13)$$

With this expression, when $er(\underline{V}_1, \underline{V}_2) = 100\%$, both vectors are orthogonal, while when $er(\underline{V}_1, \underline{V}_2) = 0\%$, both vectors are collinear. We denote by \underline{V}_{min} the eigenvector associated with the lowest eigenvalue when all eigenvalues are positive, and to the highest negative eigenvalue when at least one of them is negative. How $er(\underline{V}_{min}, \underline{dU}_f)$ evolves throughout the loading program is shown in Fig.8. It can be observed that the minimum of this function is obtained when $\det(\underline{\underline{K}}_s)$

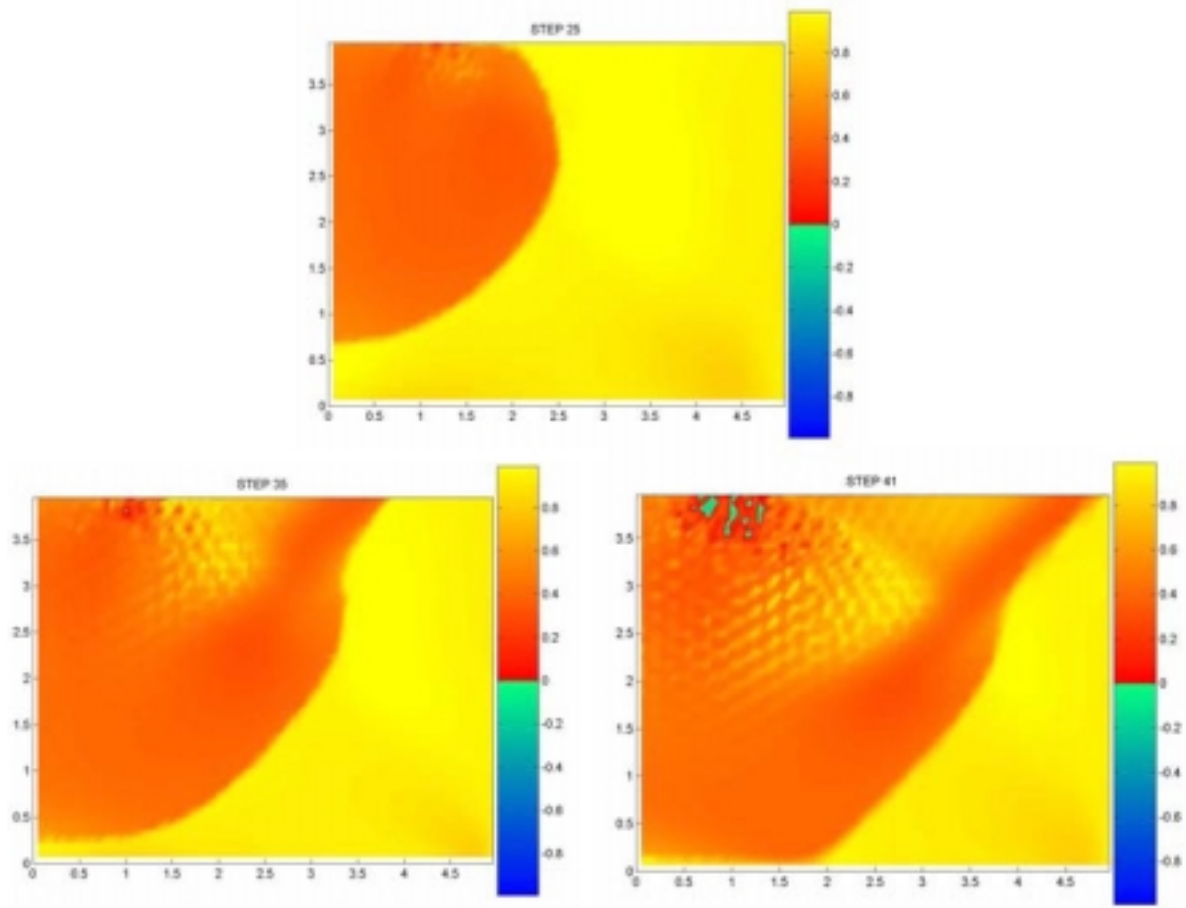


Fig. 6. Isovalues of $d^2W_n = \frac{d^2W}{\|d\sigma\| \|d\epsilon\|}$ at three characteristic computation steps: first vanishing of Λ_0 , first vanishing of d^2W_n , and divergence of the computation.

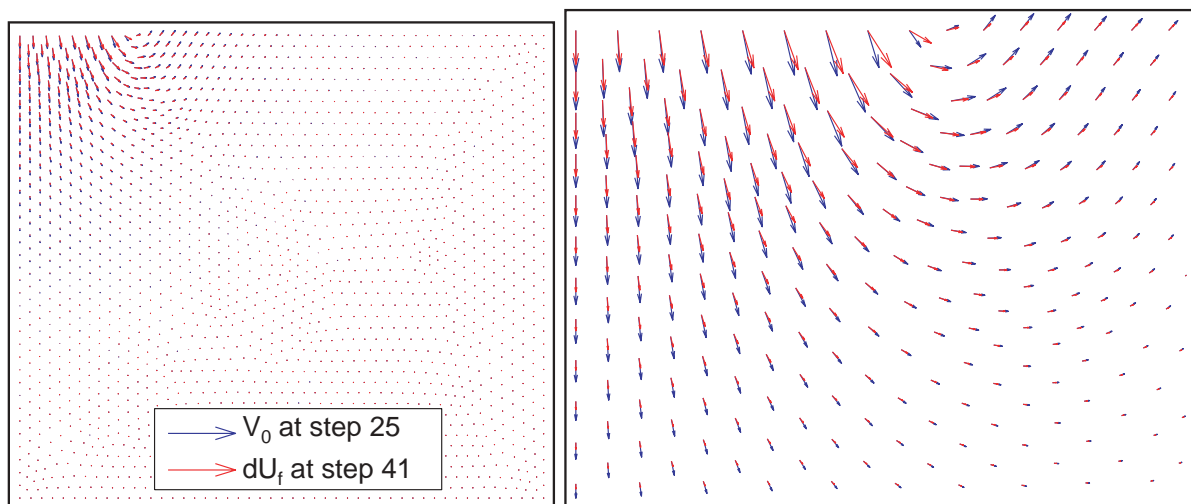


Fig. 7. \underline{V}_0 (eigenvector associated to Λ_0 , first vanishing eigenvalue) compared with \underline{dU}_f (ultimate incremental displacement field). On the right-hand side is a zoom on the zone affected by the loading conditions.

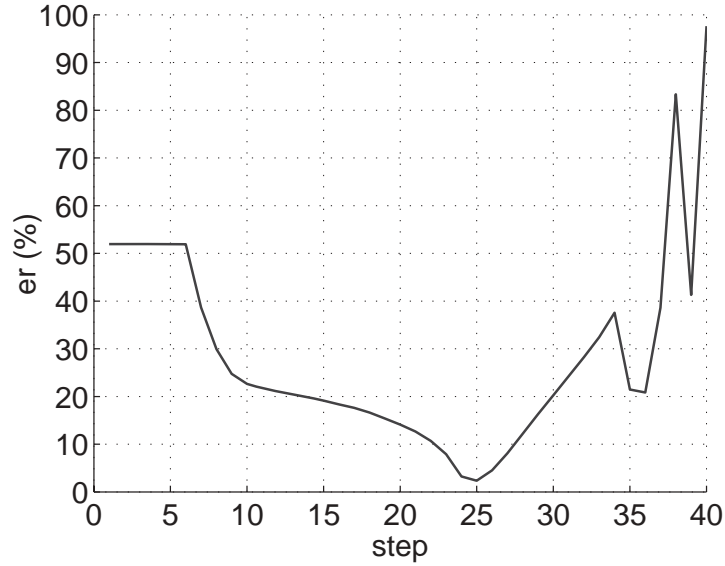


Fig. 8. $er(V_{min}, dU_f)$ evolving throughout the loading program.

vanishes.

In conclusion, the analysis of eigenvalues and eigenvectors of the symmetrical part of a global tangent stiffness matrix (\underline{K}_s) seems relevant and provides interesting information on the stability of a structure and the related nonhomogeneous failure mode.

4 CONCLUDING REMARKS

In this paper, an analysis of the second-order work criterion has been proposed at different levels, the material point levels and boundary value problem scales. As the vanishing of second-order work is related to a sudden regime transition from a static to a dynamic mode, the second-order work corresponds to a bifurcation criterion, as stated in section 2.

In the first part, the second-order work was studied in its local form. It was shown that its sign is strongly related to the changes in the eigenvalues of the symmetric part of the constitutive tensor \underline{M}_s or \underline{N}_s . When $\det(\underline{M}_s) \leq 0$, it was proved that loading directions for which $d^2W = 0$ exist and constitute a cone. Furthermore, when the second-order work vanishes on a given loading path, a peak in a plane of conjugated variables (in the second-order work sense) is reached, and a bifurcation criterion as well as a generalized flow rule can be defined according to these conjugated variables. For a given constitutive model, loading directions that lead to $d^2W = 0$ can be determined. The analytical equation of these elliptical instability cones was given for every incrementally piecewise linear model. Illustrations of these instability cones, as well as of the bifurcation domain in the 3D stress space, were presented for Darve's two constitutive models. Finally, it was shown that $\det(\underline{M}_s) = 0 \Leftrightarrow \det(\underline{N}_s) = 0$, which means that the boundary of the bifurcation domain (given by the occurrence of the first unstable direction) does not depend on the formalism chosen for the constitutive relation.

In the second part, the approach performed at the material point level was extended by analyzing the global tangent stiffness matrix stemming from a finite element simulation. The study of a soil body subjected to a flexible foundation was carried out. As shown in the past (Darve &

Laouafa 2000; Laouafa & Darve 2002), the local quantity d^2W_n accurately describes the weakness zone in the soil during the loading program. Finally, it was also observed that, qualitatively, realistic failure modes can be detected largely before the collapse for a monotonous loading program, by using the eigenvector V_0 .

As a final remark, if the question of failure in geomaterials is now well treated at the material point level, with well-established results, this is not totally the case when investigating nonhomogeneous boundary value problems. Nevertheless, the study of the properties of the eigenvalues and eigenvectors of (\underline{K}_s) seems to be promising to analyze bifurcation even in nonhomogeneous problems and particularly to characterize failure modes.

REFERENCES

- Barnichon, J.D. (1998). *Finite element modelling in structural and petroleum geology*. Ph. D. thesis, Univerité de Liège, Belgique.
- Bigoni, D. & Hueckel, T. (1991). Uniqueness and localization-i. associative and non-associative elastoplasticity. *Internationnal Journal of Solids and Structures* 28(2), 197–213.
- Darve, F. & Chau, B. (1987). Constitutive instabilities in incrementally non-linear modelling. In *Constitutive laws for Engineering Materials*, pp. 301–310. C. S. Desai.
- Darve, F., Flavigny, E., & Meghachou, M. (1995). Yield surfaces and principle of superposition revisited by incrementally non-linear constitutive relations. *International Journal of Plasticity* 11(8), 927–948.
- Darve, F. & Labanieh, S. (1982). Incremental constitutive law for sands and clays. simulations of monotonic and cyclic tests. *International Journal for Numerical and Analytical Methods in Geomechanics* 6, 243–275.
- Darve, F. & Laouafa, F. (2000). Instabilities in granular materials and application to landslides. *Mechanics of cohesive-frictional materials* 5, 627–652.
- Darve, F. & Vardoulakis, I. (Eds.) (2004). *Degradations and instabilities in geomaterials*, Volume 461 of *CISM courses*. SPRINGER.
- Hill, R. (1958). A general theory of uniqueness and stability in elasto-plastic solids. *Journal of the Mechanics and Physics of Solids* 6, 236–249.
- Hill, R. (1967). Eigenmodal deformations in elastic/plastic continua. *Journal of the Mechanics and Physics of Solids* 15, 371–386.
- Lade, P.V. (1992). Static instability and liquefaction of loose fine sandy slopes. *Journal of Geotechnical Engineering* 118(1), 51–71.
- Lagamine (2007). *User's Manual*. Département GEOMAC, Sart-Tilman B52/3, Chemin des chevreuils 1, 4000 Liège: University of Liège.
- Laouafa, F. & Darve, F. (2002). Modelling of slope failure by a material instability mechanism. *Computer and Geotechnics* 29, 301–325.
- Mandel, J. (1966). Conditions de stabilité et postulat de drcker. In J. Kravtchenko & P.M. Sirieys (Eds.), *Rheology and Soils Mechanics*, pp. 58–68. Berlin Springer.
- Mróz, Z. (1963). Non-associated flow laws in plasticity. *Journal de Mecanique* 2, 21–42.
- Mróz, Z. (1966). On forms of constitutive laws for elastic-plastic solids. *Archive of Mechanics Stosovanej* 18, 1–34.
- Nova, R. (1991). A note on sand liquefaction and soil stability. In *3rd International Conference on Constitutive Laws for Engineering Materials: Theory and Applications*, Tuscon, USA, pp. 153–156.

- Nova, R. (1994). Controllability of the incremental response of soil specimens subjected to arbitrary loading programs. *Journal of the Mechanical behavior of Materials* 5(2), 193–201.
- Prunier, F., Laouafa, F., & Darve, F. (2009). 3d bifurcation analysis in geomaterials, investigation of the second order work criterion. *European Journal of Environmental and Civil Engineering in Press*.
- Prunier, F., Laouafa, F., Lignon, S., & Darve, F. (2009). Bifurcation modeling in geomaterials: from the second-order work criterion to spectral analyses. *International Journal for Numerical and Analytical Methods in Geomechanics* DOI: 10.1002/nag.762.
- Prunier, F., Nicot, F., Darve, F., Laouafa, F., & Lignon, S. (2009). 3d multi scale bifurcation analysis of granular media. *Journal of Engineering Mechanics (ASCE) in Press*.
- Rice, J.R. (1976). The localization of plastic deformation. In W.T. Koiter (Ed.), *Theoretical and Applied Mechanics*, pp. 207–220. 14th IUTAM Congress Amsterdam.
- Van Eekelen, H.A.M. (1980). Isotropic yield surfaces in three dimensions for use in soil mechanics. *International Journal for Numerical and Analytical Methods in Geomechanics* 4, 89–101.